

Open Research Online

The Open University's repository of research publications
and other research outputs

Spectroscopic studies of ketones as a marker for patients with diabetes

Journal Item

How to cite:

Ferreira da Silva, F; Nobre, M; Fernandes, A; Antunes, R; Almeida, D; Garcia, G; Mason, Nigel and Lima-Vieira, P (2008). Spectroscopic studies of ketones as a marker for patients with diabetes. *Journal of Physics: Conference Series*, 101(012011) pp. 1–7.

For guidance on citations see [FAQs](#).

© [\[not recorded\]](#)

Version: [\[not recorded\]](#)

Link(s) to article on publisher's website:
<http://dx.doi.org/doi:10.1088/1742-6596/101/1/012011>

Copyright and Moral Rights for the articles on this site are retained by the individual authors and/or other copyright owners. For more information on Open Research Online's data [policy](#) on reuse of materials please consult the policies page.

oro.open.ac.uk

Spectroscopic studies of ketones as a marker for patients with diabetes

F Ferreira da Silva¹, M Nobre¹, A Fernandes¹, R Antunes¹, D Almeida¹, G Garcia², N J Mason³ and P Limão-Vieira^{1,3}

1 Atomic and Molecular Collisions Laboratory, CEFITEC, Department of Physics, New University of Lisbon, 2829-516 Caparica, PORTUGAL

2 Instituto de Matemáticas y Física Fundamental, Consejo Superior de Investigaciones Científicas (CSIC), Serrano 113-bis, 28006 Madrid, SPAIN

3 Department of Physics and Astronomy, The Open University, Walton Hall, Milton Keynes, MK7 6AA, UK

Email: plimaovieira@fct.unl.pt

Abstract. Acetone in human breath has been established as a biomarker for diabetes. The application of UV spectroscopy for the study of biomedical compounds has been developed over recent years but is often limited by the lack of absolute data for calibration of the instrumentation. By measuring high resolution absolute VUV photoabsorption cross sections of acetone, we are able to provide calibration values at several wavelengths with special attention to 4.661 eV (266 nm). Results are compared with recent published data [C Wang, A Mbi, Meas. Sci. Technol., 2007, **18**, 2731–2741]. The acetone spectrum is here revisited from a recent contribution [Nobre M, *et al*, *Phys Chem Chem Phys*, 2008 (in press)] where the absolute cross sectional values are obtained in the 3.7 – 10.8 eV energy region. Future medical units working in close link with synchrotron radiation facilities can make use of the VUV spectra wavelength region to trace acetone in diabetic patients.

1. INTRODUCTION

Healthy human breath contains hundreds of volatile organic compounds (VOCs) albeit in very low concentrations - from a few pptv (part-per-trillion volume) to ppbv (part-per-billion volume) levels [1]. Very recently some of these VOCs have been identified as biomarkers to some specific diseases and/or pathologies, e.g., alkanes are present in patients with lung cancer, formaldehyde is detected in patients suffering from breast cancer [2, 3], isoprene is an indication of high blood cholesterol levels [4] and type-1 diabetes (T1D) is linked to the presence of acetone [5, 6]. Hence breath analysis may be very useful in diagnosing human diseases [7]. However, due to the low concentrations and presence of a large number of chemical species in exhaled breath, breathe analysis requires high sensitive and selective instrumentation to detect and identify the atypical concentrations of specific biomarkers. Several experimental techniques have been used such as: Gas Chromatography-Mass Spectrometry (GC-MS) [8], which is a sensitive and accurate method but still requires yet sample preparation by means of complicated procedures. Selection Ion Flow Tube-Mass Spectrometry (SIFT-MS) [9], does

not require previous gas chromatography separation but the quantification and accuracy of this technique depend on the knowledge of the rate constants of the reactions examined. Very recently the Light Emitting Diode (LED)-based photometric method has been applied to the detection of acetone in the human breath [7]. This has proven to be an affordable approach but requires a sophisticated calibration procedure to obtain absolute concentrations of acetone. There are other potential breath analysers based on electrical sensors [10] or nondispersive infrared (NDIR) sensors [11], which are comparatively less expensive and smaller in size but operate with considerably low sensitivity. Wang and Mbi [12] have developed a breath analyser for diabetes using a Cavity Ringdown Spectroscopy (CRDS) method at a single wavelength of 266 nm (4.661 eV) that has shown to be high sensitive, leading to absolute measurements of gas concentration of species of interest and also recognized to be an ideal technique for real-time, non-invasive analysis. A recent publication from Gunasekaran and Sakari [13] in the study of biomedical compounds, such as blood, has shown that with the onset of a disease, the relative content of the biomolecules of blood changes, producing pathophysiological modifications that can be traced by application of spectroscopic techniques as a diagnostic tool in clinical chemistry. Though, this approach can also be an alternative method in clinical analysis. Such evidence has been reported recently by making use of FTIR and UV-Vis spectroscopies to show spectral differences between a normal healthy serum and that affected with a diabetic pathology [13].

In humans and most other mammals, the oxidation process of fatty acids in the liver can lead to a known citric acid cycle [14] or undergo conversion to the production of the so called ketone bodies, acetone, acetoacetate and d- β -hydroxybutyrate that are thereafter delivered to other tissues. In healthy people, acetone is produced in minor quantities from acetoacetate, which is easily decarboxylated, either spontaneously or to a lesser extent by enzymatic conversion of acetoacetate decarboxylase. Patients with untreated diabetes produce large amounts of acetoacetate in their blood stream such that one can find significant amounts of acetone, which has been found to be toxic. Acetone is volatile and imparts to these individuals a very peculiar odour to their breath (commonly known as 'sweet odour'), which may be used in diagnosing diabetes. Untreated diabetes (e.g., mellitus) leads to the overproduction of ketone bodies, producing several other medical conditions, and when the insulin level is not enough, extrahepatic tissues cannot take up glucose efficiently from the blood, either for fuel or for fat conversion. The accelerated formation of ketones is beyond the capacity of extrahepatic tissues to oxidise them and as a result leads to lowering of the blood pH, causing acidosis. Extreme acidosis can lead to coma and in some cases to death.

Acetone, $(\text{CH}_3)_2\text{CO}$, is the simplest carbonyl and aliphatic compound that has been extensively studied as a model for the ketone family. Acetone concentration in healthy humans breath gas shows a large distribution ranging from a few ppbv to 2 ppmv and the average concentration is within the range of 0.79 – 1.4 ppmv based on very recent measurements using mass spectrometric based techniques and broadband LED absorption spectroscopy [7, 15 – 17]; however, acetone levels can rise as much as 12 ppmv in acute diabetes [18].

Exposure investigations of golden hamsters to 350 Gy of X-Rays have shown that the induction of acute and specific necrosis of the pancreas is observed within a few hours, whereas no other tissue revealed any drastic changes which would lead to a critical pathology until 36 hours after exposure [19]. Animals began to show characteristic signs of diabetes with the production of high levels of ketone bodies (ketosis) and acidosis, which would lead to death several hours after. In order to quantify the risk of radiation damage several models have been developed to study the effect of radiation on cellular material. Such models require a detailed understanding of the underlying interactions between the primary radiation and the cellular environment, indeed recent experiments have demonstrated that secondary electrons may in fact driven much of the radiation chemistry [20]. Our understanding of radiation damage within cells, and thence mutagenesis, therefore depends upon our detailed knowledge of the spectroscopy and dissociation dynamics of key components in certain initiation reactions.

In this paper we are particularly interested in the acetone electronic state spectroscopy since this may be used as a fingerprint for spectroscopic detection of acetone in breath analysis. Several

experimental [21 – 37] and theoretical [38 – 40] studies on the electronic state spectroscopy of acetone have been reported and recently high resolution VUV photoabsorption spectroscopy in the energy range 3.7 – 10.8 eV has been obtained [41]; new vibronic structure has been observed, notably in the low energy absorption band assigned to the $1^1A_1 \rightarrow 1^1A_2$ ($n_y \rightarrow \pi^*$) transition. The local absorption maximum at 7.85 eV has been tentatively attributed to the 4^1A_1 ($\pi \rightarrow \pi^*$) transition. Six Rydberg series converging to the lowest ionisation energy (9.708 eV) have been assigned as well as a newly-resolved *ns* Rydberg series converging to the first ionic excited state (12.590 eV). Rydberg orbitals of each series have been classified according to the magnitude of the quantum defect (δ) and extended to higher quantum numbers than in the previous analyses. In this paper we report revised data from a recent contribution [41] that provides a summary of this data and recommend absolute cross sections. The energy range covered in the present work (3.7 – 10.8 eV), from where future medical units working in close link with synchrotron radiation facilities, can make use of the VUV spectra energy (wavelength) region to trace acetone in diabetic patients in a extended region than in previous reported contributions [12].

2. EXPERIMENTAL PROCEDURE

High-resolution VUV photoabsorption spectra of acetone (Fig. 1) were recorded on the UV1 beam line of the ASTRID synchrotron facility at the University of Aarhus, Denmark. The experimental apparatus has been described in detail elsewhere [42]. Synchrotron radiation was passed through a static gas sample and a photomultiplier was used to measure the transmitted light intensity. The incident wavelength was selected using a toroidal dispersion grating with 2000 lines/mm providing a resolution of ~ 0.075 nm at FWHM, corresponding to approximately 1 meV for 4.5 eV incident photons and 6 meV at 10 eV. The step size in the data collection was always chosen to be less than the resolution.

For wavelengths below 200 nm, helium gas was flushed through the small gap between the photomultiplier and the exit window of the gas cell to prevent any absorption by oxygen in the nascent air contributing to the spectrum. The wavelength range used, 115 – 330 nm (10.8 – 3.7 eV), was determined by the windows of the gas cell (LiF entrance and CaF₂ exit) and the grating respectively. To avoid any saturation effects, sample pressures were chosen to ensure that the transmitted flux was $> 10\%$ of the incident flux [43] and were typically in the range 0.023 – 0.938 Torr, measured using a capacitance manometer (Baratron). The synchrotron beam ring current was monitored throughout the experiments and each sample measurement was accompanied by a background scan recorded with the cell evacuated. Absolute photoabsorption cross sections were obtained using the Beer-Lambert attenuation law:

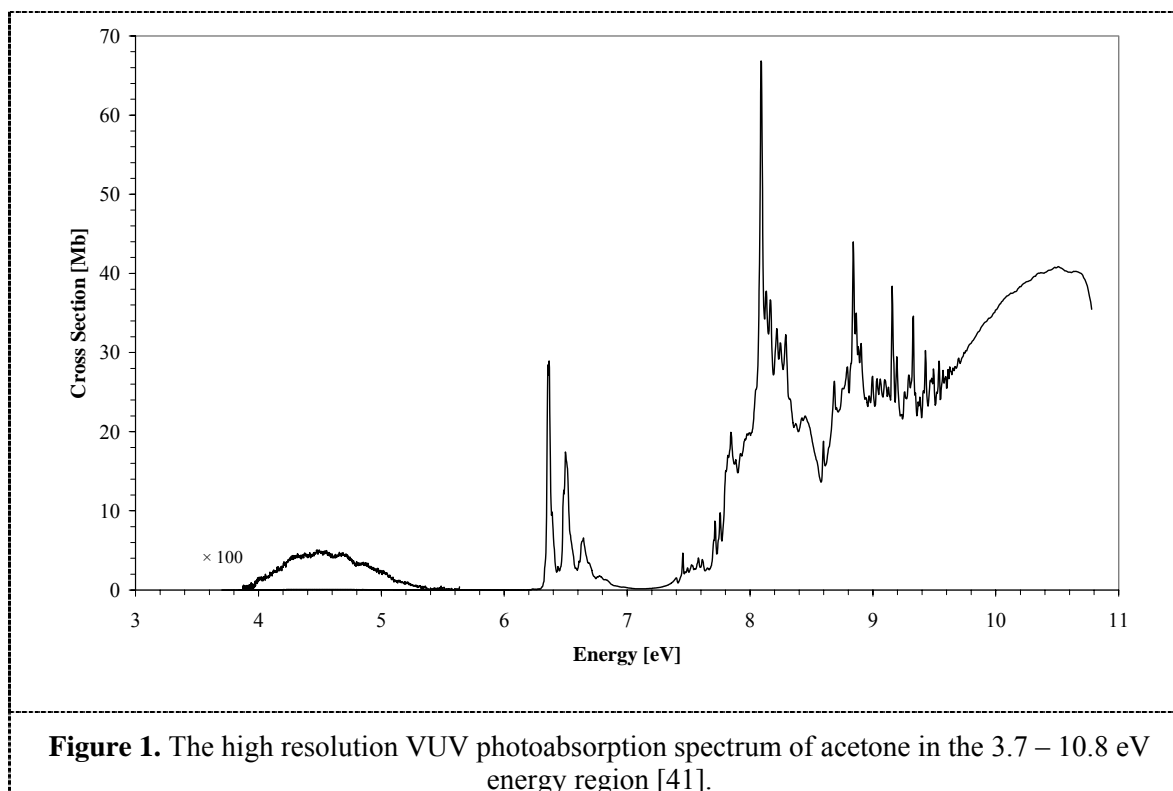
$$I_t = I_0 \exp(-n\sigma x)$$

where I_t is the radiation intensity transmitted through the gas sample, I_0 is the radiation intensity transmitted through the evacuated cell, n is the molecular number density of the sample gas, σ the absolute photoabsorption cross section, and, x is the absorption path length (25 cm). The accuracy of the cross-section is estimated to be $\pm 5\%$ in agreement with previous estimates made by Eden *et al.* [42] and Giuliani *et al.* [44]. However, the percentage error increases when absorption by the sample gas is very weak ($I_t \approx I_0$). In this case, the level of noise on the measured cross section gives the best indication of the error.

The liquid sample used in the VUV measurements was purchased from Sigma-Aldrich with a minimum purity of 99.8%. The sample was degassed by repeated freeze–pump–thaw cycles.

3. RESULTS AND DISCUSSION

The absolute high resolution VUV photoabsorption spectrum of acetone is shown in Figure 1 from 3.7 to 10.8 eV. The observed absorption bands have been classified either as members of Rydberg series or molecular valence transitions of the type ($n_y \rightarrow \pi^*$), ($n_y \rightarrow \sigma^*$), ($\sigma \rightarrow \pi^*$) and ($\pi \rightarrow \pi^*$) [35 – 39]. The first Rydberg state arises from the $3s(b_2) \leftarrow 5b_2(n_y)$ ($1^1B_2 \leftarrow 1^1A_1$) transition and has a maximum cross section of $29 \pm 2 \text{ Mb}^1$ at 6.365 eV, in good agreement with recent work [36].



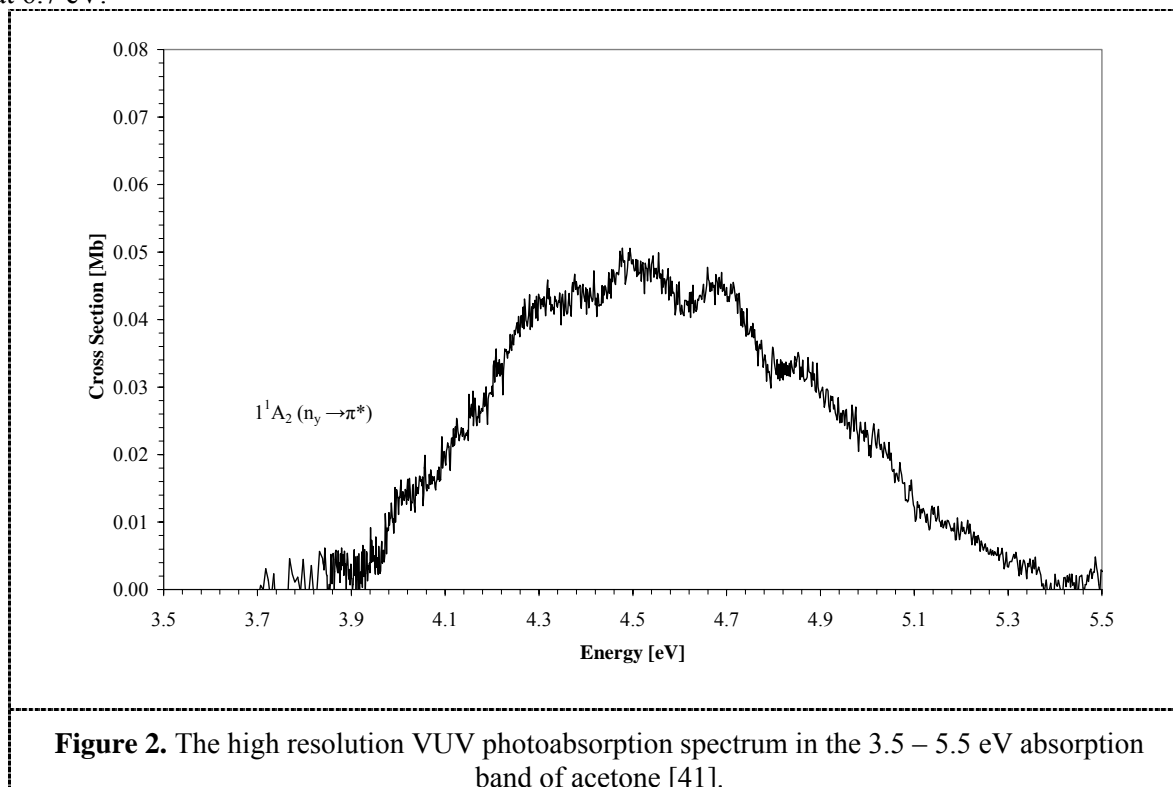
3.1 Energy region 3.5 – 5.5 eV

Recent VUV photoabsorption [41] have confirmed previous electron scattering [29, 31, 32] studies of a dipole forbidden band at ~ 4.5 eV. This has been identified as a $3b_1(\pi^*) \leftarrow 5b_2(n_y)$ ($1^1A_2 \leftarrow 1^1A_1$) transition from the non-bonding electrons on the oxygen atom lone pairs to the first π anti-bonding molecular orbital. In the present high resolution VUV spectrum we observed local maxima cross sections of $0.051 \pm 0.003 \text{ Mb}$ at 4.494 eV (Figure 2) and a $0.046 \pm 0.003 \text{ Mb}$ at 4.461 eV. Photolysis experiments [32] suggest that the predominant dissociative process in this energy region leads to the production of $\text{CH}_3\text{CO} + \text{CH}_3$; these highly reactive radicals can undergo a complex chemistry forming secondary hydrocarbon species.

3.2 Energy region 6.2 – 7.0 eV

¹ $1\text{Mb} = 1 \times 10^{-18} \text{ cm}^2 = 1 \times 10^{-22} \text{ m}^2$

The valence band in this energy range has been assigned to the $B \leftarrow \tilde{X}^1A_1$ transition in agreement with Huebner *et al.* [29]. The $(0 - 0)$ transition has been identified at 6.355 eV [41]. This energy region shows a local maximum in the cross section of 28.934 Mb at 6.365 eV. Photodissociation in this energy region leads to $(CH_3)_2CO^* \rightarrow 2CH_3 + CO$ with a quantum yield of 1.0 for CO production at 6.7 eV.



3.3 Energy region 7.1 – 8.1 eV

In this energy region the absorption spectrum includes bands which have been attributed to three distinct electronic states at 7.400, 7.454, 7.715 and 8.090 eV [41]. The local maximum in the cross section had a value of 66.841 ± 0.005 Mb and is found at 8.090 eV.

3.4 Energy region 8.0 – 10.8 eV

Recent studies of Merchán *et al.* [38] predict the vertical excitation energy of the 2^1B_1 valence excited state at ~ 9.10 eV above the ground state and the $(\sigma \rightarrow \pi^*)$ transition to have a similar oscillator strength to the $(n_y \rightarrow 3s)$ transition [41]. In this energy region we observe a local maximum cross section of 38.382 ± 0.005 Mb at 9.157 eV. Huebner *et al.* [29] have reported four important primary dissociation mechanisms with particular attention to those leading to the production of H, $CH_2CO + CH_3$, and $CO + 2CH_3$; hydrogen atom loss should occur at 7.9 eV following excitation of a $(\pi \rightarrow \pi^*)$ transition [41]. The reaction leading to the production of hydrogen radicals seems to be extremely important in physiological conditions since it can be close related to the lowering of pH in the blood that may lead to acidosis in diabetic patients. However, the mechanism for such reactions in the biological environment is likely to be complex.

4. ABSOLUTE CROSS SECTIONS

The present absolute cross section values for acetone in the energy range 3.7 – 10.8 eV are revisited and, as far as we are aware, are the highest resolution data yet reported [41]. Wang and Mbi [12] have

used a cross sectional value for acetone at atmospheric pressures of $4.50 \times 10^{-20} \text{ cm}^2$ at a wavelength of 266 nm (4.661 eV) to calibrate their optical detection system and these in good agreement with the value of $4.59 \times 10^{-20} \text{ cm}^2$ determined in the present measurements.

5. CONCLUSIONS

The cross sectional value at 266 nm (4.661 eV) used by Wang and Mbi [12], has allowed to derive a detection limit in their experiment of 0.49 ppmv. However, as these authors discussed, there are several limitations arising from calibrating measurements at this wavelength (266 nm) especially since the detection limit is lower than the average acetone concentration in normal human breath gas, 0.79 – 1.4 ppmv. Therefore, with the present broad energy absorption range (3.7 – 10.8 eV) and future medical units working in close link with synchrotron radiation facilities, it should be possible to use the VUV photoabsorption spectra to trace acetone in diabetic patients by calibration in other absorption regions with higher intensities (higher cross sections). Since acetone is a very important physiologic metabolic marker in human breath and therefore knowing the accurate levels of it is extremely important from the point of view of diagnosing diabetes we believe the data reported in this paper will therefore provide such an alternative calibration procedure for the clinical community.

ACKNOWLEDGMENTS

MN, AF and DA acknowledge the support from the EU network RADAM and RA the Portuguese Foundation for Science and Technology (FCT-MCTES) for a post-graduate scholarship. PLV acknowledges the visiting research fellow position at CEMOS, The Open University, UK, and together with NJM, the support from the British Council for the Portuguese-UK joint collaboration. The authors wish to acknowledge the beam time at the ISA synchrotron facility, University of Aarhus, Denmark, I3 Integrated Activity on Synchrotron and Free Electron Laser Science (IA-SFS), contract number RII3-CT-2004-506008, under the Research Infrastructure Action of the FP6 EC programme Structuring the European Research Area. Some of this work forms part of the ESF network programme EIPAM and EU/ESF RADAM COST Action-P9.

References

- [1] Pauling L, Roinson A B, Teranishi R, Cary P, *Proc Nat Acad Sci*, 1971, **68**, 2374–2376.
- [2] O'Neill H J, Gordon S M, O'Neill M H, Gibbons R D, Szidon J P, *Clin Chem*, 1988, **34**, 1613–1618.
- [3] Gordon S M, Szidon J P, Krotoszynski B K, Gibbons R D, O'Neill H J, *Clin Chem*, 1985, **31**, 1278–1282.
- [4] Karl T, Prazeller P, Mayr D, Jordan A, Rieder J, Fall R, Lindinger W, *J Appl Physiol*, 2001, **91**, 762–770.
- [5] Manolis A, *Clin Chem*, 1983, **29**, 5–15.
- [6] Musa-Veloso K, Rarama E, Comeau F, Curtis F, Cunnane S, *Pediatr Res*, 2002, **52**, 443–448.
- [7] Teshima N, Li J, Toda K, Dasgupta P K, *Anal Chim Acta*, 2005, **535**, 189–199.
- [8] Joachim D P, Andrew B, *Clin Chem*, 1997, **43**, 723–730.
- [9] Turner C, Spanel P, Smith D, *Physiol Meas*, 2006, **27**, 321–327.
- [10] Ryabtsev SV, Shaposhnick AV, Lukin A N, Domashevskaya E P, *Sens Actuators B*, 1999, **59**, 26–29.
- [11] Braden B, Schaefer F, Caspary W F, Lembcke B, *Scand J Gastroenterol*, 1996, **31**, 442–445.
- [12] Wang C, Mbi A, *Meas Sci Technol*, 2007, **18**, 2731–2741.
- [13] Gunasekaran S, Sankari G, *Asian J Chem*, 2004, **16**, 1779–1786.
- [14] D. L. Nelson and M. M. Cox, *Principles of Biochemistry*, 4th Ed., W. H. Freeman & Company,

New York, 2005.

- [15] Deng C, Zhang J, Yu X, Zhang W, Zhang X, *J Chromatogr*, 2004, **810**, 269–275.
- [16] Diskin A M, Spanel P, Smith D, *Physiol Meas*, 2003, **24**, 107–120.
- [17] Andersen J C, Lamm W J E, Hlasatala M P, *J Appl Physiol*, 2005, **100**, 880–889.
- [18] Mueller W, Schubert J, Benzing A, Geiger K, *J Chromatogr B*, 1998, **716**, 27–38.
- [19] Tsubouchi S, Suzuki H, Ariyoshi H, Matsuzawa T, *Int J Rad Bi.*, 1981, **40**, 95–106.
- [20] Boudaïffa B, Cloutier P, Hunting D, Huels M A, Sanche L, *Science*, 2000, **287**, 1658–1660.
- [21] Noyes Jr W A, Duncan A B F, Manning W M, *J Chem Phys*, 1934, **2**, 717–725.
- [22] Duncan A B F, *J Chem Phys*, 1935, **3**, 131–132.
- [23] McMurry H L, *J Chem Phys*, 1941, **9**, 231–240.
- [24] Lawson M, Duncan A B F, *J Chem Phys*, 1944, **12**, 329–335.
- [25] Holdsworth R S, Duncan A B F, *Chem Rev*, 1947, **41**, 311–316.
- [26] Watanabe K, *J Chem Phys*, 1954, **22**, 1564–1570.
- [27] Lake J S, Harrison A J, *J Chem Phys*, 1959, **30**, 361–362.
- [28] Barnes E F, Simpson W T, *J Chem Phys*, 1963, **39**, 670–675.
- [29] Huebner R H, Cellota R J, Mielczarek S R, Kuyatt C E, *J Chem Phys*, 1973, **59**, 5434–5443.
- [30] Baba M, Hanazaki I, Nagashima U, *J Chem Phys*, 1985, **82**, 3938–3947.
- [31] Walzl K N, Koerting C F, Kuppermann A, *J Chem Phys*, 1987, **87**, 3796–3803.
- [32] St. John III W M, Estler R C, Doering J P, *J Chem Phys*, 1974, **61**, 763–767.
- [33] McDiarmid R, *J Chem Phys*, 1991, **95**, 1530–1536.
- [34] Furuya K, Katsumata S, Kimura K, *J Electron Spectrosc Relat Phenom*, 1993, **62**, 237–243.
- [35] Xing X, McDiarmid R, Phils J G, Goodman L, *J Chem Phys*, 1993, **99**, 7565–7573.
- [36] McDiarmid R, Xing X, *J Chem Phys*, 1997, **107**, 675–679.
- [37] ter Steege D H A, Wirtz A C, Bruma W J, *J Chem Phys*, 2002, **116**, 547–560.
- [38] Merchán M, Roos B O, McDiarmid R, Xing X, *J Chem Phys*, 1996, **104**, 1791–1804.
- [39] Liao D W, Mebel A M, Hayashi M, Shiu Y J, Chen Y T, Lin S H, *J Chem Phys*, 1999, **111**, 205–215.
- [40] Borges Jr I, Rocha A B, Bielschowsky C E, *Braz J Phys*, 2005, **35**, 971–980, and references therein.
- [41] Nobre M, Fernandes A, Ferreira da Silva F, Antunes R, Almeida D, Kokhan V, Hofmann S V, Mason N J, Eden S, Limão-Vieira P, *Phys Chem Chem Phys*, 2008, DOI: 10.1039/b708580j.
- [42] Eden S, Limão-Vieira P, Hoffmann S V, Mason N J, *Chem Phys*, 2006, **323**, 313–333.
- [43] Mason N J, Gingell J M, Davis J A, Zhao H, Walker I C, Siggel M R F, *J Phys B*, 1996, **29**, 3075–3089.
- [44] Giuliani A, Delwiche J, Hoffmann S V, Limão-Vieira P, Mason N J, Hubin-Franskin M-J, *J Chem Phys B*, 2003, **119**, 3670–3680.